# Metal Inhibition of Human Alkylpurine-DNA-*N*-glycosylase Activity in Base Excision Repair

Ping Wang[†], Anton B. Guliaev[†], and Bo Hang*

Department of Molecular Biology, Life Sciences Division,

Lawrence Berkeley National Laboratory,

University of California,

Berkeley, CA 94720

Running title:

**Inhibition of Human APNG by Metals**

*To whom correspondence should be addressed: Tel: 510-495-2537. Fax: 510-486-6488. E-mail: Bo_hang@lbl.gov**.**

[†]Both authors contributed equally.

Abbreviations: $Cd^{2+}$, cadmium; $Ni^{2+}$, nickel; $Zn^{2+}$, zinc; APNG, alkylpurine-DNA-*N*-glycosylase; Fpg, formamidopyrimidine-DNA glycosylase; OGG1, 8-oxoG-DNA glycosylase; AP, apurinic/apyrimidinic; APE1, AP endonuclease 1; BER, base excision repair; NER, nucleotide excision repair; MMR, mismatch repair; εA, 1,$N^6$-ethenoadenine; THF, tetrahydrofuran; MD, molecular dynamics

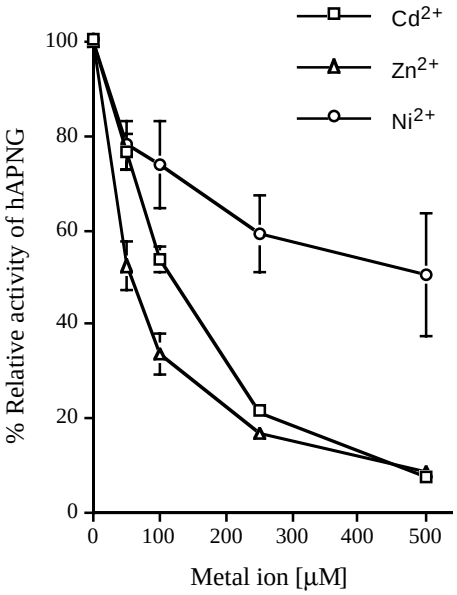
Cd2+
Zn2+
Ni2+
% Relative activity of hAPNG
100
80
60
40
20
0
0
100
200
300
400
500
Metal ion [µM]

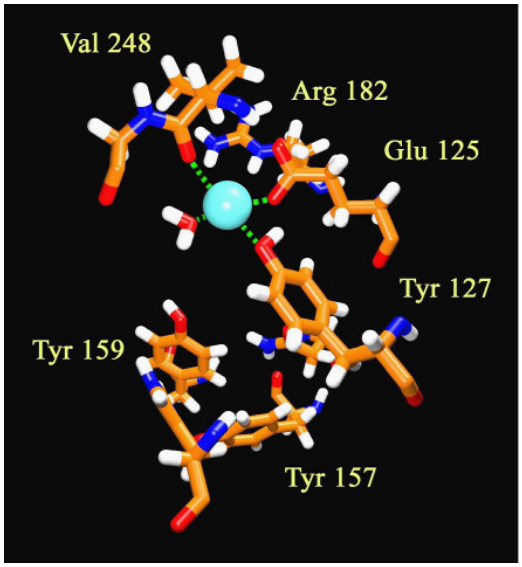
Val 248
Arg 182
Glu 125
Tyr 127
Tyr 159
Tyr 157

**Abstract**

Both cadmium ($Cd^{2+}$) and nickel ($Ni^{2+}$) are established environmental human carcinogens without physiological functions found so far. Zinc ($Zn^{2+}$) is not listed as a carcinogen, and rather an essential element to humans. Metal ions have recently been shown to inhibit a number of DNA repair proteins that use metals for their function and/or structure. In this study, we report that $Cd^{2+}$, $Ni^{2+}$, and $Zn^{2+}$ are able to inhibit the activity of a recombinant human alkylpurine-DNA-*N*-glycosylase (hAPNG) towards a DNA oligonucleotide containing a 1,$N^6$-ethenoadenine (εA). This enzyme displays a broad substrate specificity and does not require metal for its catalytic activity or structural integrity. At concentrations starting from 50 to 1000 μM, both $Cd^{2+}$ and $Zn^{2+}$ showed metal-dependent inhibitory effects on hAPNG catalytic activity. $Ni^{2+}$ also inhibited the enzyme activity, but to a lesser extent. Studies using HeLa cell-free extracts demonstrated similar patterns of inactivation of the εA excision activity by the same metals. When a gel mobility shift assay was used, binding of hAPNG to the substrate was not significantly affected by $Cd^{2+}$ at concentrations that strongly inhibit the catalytic function, suggesting that the reduced glycosylase activity is not due to altered APNG binding affinity to the substrate. In this study we also applied molecular dynamics (MD) simulations to gain insight into potential interactions between metal ion and the hAPNG active site. Simulations using $Zn^{2+}$ showed that the hAPNG active site could have a $Zn^{2+}$ binding site, formed by several catalytically important and conserved residues. Metal binding to such a site is expected to interfere with the catalytic mechanism of this protein. These data suggest that inhibition of hAPNG activity may contribute to metal mutagenicity, and could be the basis for the previously reported metal inhibition of repair of alkylating agents-induced DNA damage in cells.

## Introduction

In addition to multiple toxic effects from excessive exposure, many metals and their compounds have been found to cause cancer in experimental animals and/or humans. Two of the common toxic metals are cadmium ($Cd^{2+}$) and nickel ($Ni^{2+}$), which have no physiological functions found to date. Exposure to these two metals and their compounds has been an occupational hazard for a large number of workers involved in a variety of related industrial fields (*1-3*). Given that both are ubiquitous in the environment and are widely used in consumer products, the general population can be exposed through multiple routes including food, water, air and skin contact (*1-3*). Environmental exposure to cadmium is mostly through tobacco smoke for smokers and through food for non-smokers. Environmental pollution of cadmium also includes other sources such as fuel combustion, nickel-cadmium batteries and contaminated soil. For nickel, although inhalation occurs, the general population is mainly exposed through food. Dermal contact with nickel alloys and other nickel products is also a route of exposure. Unlike these two metals, zinc ($Zn^{2+}$) is an essential element for numerous cellular proteins and normal metabolic mechanisms, as well as for cell growth and division (*4*). However, over exposure to this metal, resulting from occupational exposure or therapeutic administration, can lead to a variety of toxic symptoms in both humans and animals (*5*).

Both cadmium and nickel are classified as human carcinogens by the International Agency for Research on Cancer (IARC) (*2, 3*) and the National Toxicology Program (NTP) (*1*). Exposure to cadmium and its compounds has been associated with increased cancer risk in human lung, prostate and testis (*1, 2*). Animal experiments support that cadmium is a potent carcinogen as it induces malignancies in multiple organs including lung, prostate, liver and kidney, as well as at sites of injection, depending on the route of exposure (*1, 2*). Likewise, nickel and its compounds are related to increased risk of lung and nasal cancer in exposed workers and induce tumors in various organs of experimental animals, such as lung, liver and kidney (*1, 3*). It is believed that the ionic form of metals in their compounds is the active biological species. To date, although possible carcinogenicity of zinc has been investigated through animal experiments and occupational exposure, no sufficient evidence supports such a link.

Despite that the carcinogenicity of both cadmium and nickel has long been established, the mechanisms by which they promote cancer transformation remain unclear. A number of mechanisms have been proposed, including both genotoxic and epigenetic effects of these metals on target cells. Recent evidence also points to that inhibition of DNA repair processes is an important mechanism responsible for metal induced mutagenesis and carcinogenesis (*6-9*). DNA repair is an essential cellular mechanism for maintaining genomic integrity and its capacity is considered a crucial

determinant of cancer susceptibility (*10, 11*). It contains several major pathways, including base excision repair (BER), nucleotide excision repair (NER), and mismatch repair (MMR), with each recognizing and repairing different types of DNA damage. Studies on effects of metal ions showed both *in vivo* inhibition of repair of DNA damage caused by specific agents and *in vitro* inactivation of individual enzymes in these repair pathways. The target proteins identified include the NER component xeroderma pigmentosum group A protein (XPA) (*12, 13*), the MMR recognition unit MSH2-MSH6 complex (*14, 15*), and several core enzymes in BER (*16-19*). In general, if metal inactivates a DNA repair enzyme, cells would accumulate unprocessed mutagenic DNA lesions or reaction intermediates that are normally processed by the enzyme, thereby enhancing the genotoxicity of other DNA damaging agents, either from exogenous or endogenous sources.

The BER pathway repairs a wide range of modified bases including alkylated, oxidized and deaminated derivatives (*10*). It is initiated by damage-specific DNA glycosylases that hydrolyze the glycosylic bond between a modified base and sugar, generating an apurinic/apyrimidinic (AP) site. In the simplistic pathway of BER, AP site is cleaved by AP endonuclease 1 (APE1), followed by DNA polymerase β (POLβ) which removes the abasic sugar (dRpase activity) and fills the single nucleotide gap (DNA polymerase activity). A DNA ligase seals the nick. Metals have been shown to inhibit

cellular removal of both oxidative and alkylation DNA damage (*20-23*), which are primarily repaired by the BER pathway. Two glycosylases that excise oxidized bases, the bacterial formamidopyrimidine-DNA glycosylase (Fpg) and the murine 8-oxoG-DNA glycosylase (mOGG1), are found to be targets for several metal ions (*12, 16*). Recently it was also found that the human APE1 nuclease activity is inhibited by lead ($Pb^{2+}$), iron ($Fe^{2+}$) and $Cd^{2+}$ (*17*). In addition, POLβ and poly(ADP-ribose) polymerase-1 (PARP-1) are both inactivated by $Cd^{2+}$ and other metals (*18, 19, 24*). To date, the studies on metal-protein interactions in repair have mainly been focused on those zinc finger proteins (*e.g.* XPA, Fpg and PARP-1) and other metal-requiring enzymes (*e.g.* APE1, ATPase of MSH2-MSH6).

In this work, we were interested in whether the activity of the human alkylpurine-DNA-*N*-glycosylase (APNG, also AAG and MPG) could also be affected by metal ions. If so, what would be the possible mechanism for the metal-hAPNG interactions? Unlike the proteins mentioned above, to our knowledge, hAPNG does not require a metal for its function or structure. This is a well characterized enzyme with a broad substrate specificity, excising a number of alkylated, exocyclic and deaminated bases formed by exogenous agents or by endogenous processes (*25-27*). hAPNG and its homologues in other species are known to function in mutation avoidance (*26, 27*). Its mechanism of action has been proposed based on co-crystal structures (*28, 29*), in which a base flipping

strategy is employed to dock a target base into the active site pocket. The catalytic reaction is achieved through the active site bound water molecule, which is deprotonated by nearby Glu125 to form a nucleophile for the attack on the C1' of the sugar, resulting in base release. In this study, we found that $Cd^{2+}$, $Ni^{2+}$ and $Zn^{2+}$ at their micromolar concentrations inhibit the activity of a recombinant hAPNG, or human cell-free extracts, against DNA containing a 1,$N^6$-ethenoadenine (εA). In addition, we used molecular dynamics (MD) simulations to study the potential interactions between $Zn^{2+}$ and hAPNG, which revealed the $Zn^{2+}$ affinity towards several catalytically important and conserved residues in the hAPNG active site.

## Experimental Procedures

**Caution:** *Cadmium and nickel compounds are classified carcinogens and should be handled with appropriate protection in accordance with NIH guidelines.*

**Chemicals, Proteins and Synthetic Oligonucleotides**. Cadmium chloride ($CdCl_2$), nickel chloride ($NiCl_2$), and zinc chloride ($ZnCl_2$) were all purchased from Aldrich-Sigma (St. Louis, MO). Stock solutions at 0.1 mM concentration were prepared using distilled and deionized water obtained from the Millipore ultrapurification system. Cell-free extracts from HeLa S3 cells (Cell culture Center, Endotronics, Minneapolis, MN) were

prepared as described previously (*30*). Truncated human recombinant protein APNG was a generous gift from Dr. T.R. O'Connor (Beckman Research Institute, CA). Recombinant hAPE1 was obtained from Enzymax (Lexington, KY). The 25-mer oligonucleotide containing a single εA at 6$^{th}$ position from the 5' side (5'-CCGCTεAGCGGGTACCGAGCTCGAAT) was synthesized as described previously (*31*). For an AP site-containing substrate, the same 25-mer sequence as above was synthesized with a tetrahydrofuranyl (THF) residue at the 8$^{th}$ position by Operon, Inc. (Alameda, CA). The complementary strand and the 5-mer and 7-mer size markers were synthesized either with an Applied Biosystems Model 394 automated DNA synthesizer or purchased from Operon. All modified and unmodified oligomers were HPLC- and/or PAGE-purified.

**DNA Binding Assay**. To prepare a radiolabeled DNA substrate, the εA-containing 25-mer oligonucleotide was 5'-end labeled with [γ-$^{32}$P] ATP (specific activity 6,000 Ci/mmol; 1 Ci = 37 GBq, Amersham Pharmacia Biotech, Piscataway, NJ) and T4 polynucleotide kinase (United States Biochemical, Cleveland, OH) according to standard procedure. The $^{32}$P-labeled oligomer was subsequently annealed to a complementary strand in a molar ratio of 1:1.5 by slow cooling from 80$^{o}$C to room temperature. A gel mobility shift assay described previously (*30*) was used to measure the binding activity of

hAPNG for the εA-containing DNA duplex in the presence of $CdCl_2$. Briefly, the standard binding reactions contained 10 mM HEPES-KOH (pH 7.4), 100 mM KCl, 0.1 mM DTT, 10% glycerol, and 140 nM purified hAPNG in a total volume of 10 μl. $CdCl_2$ was added to the system in two different ways: (1) Pre-incubation of hAPNG with $CdCl_2$ on ice for 10 min before adding the 5'-end $^{32}$P-labeled duplex DNA (2 nM). The final reaction mixture was incubated for 15 min at room temperature (~20 °C); (2) Incubation of hAPNG and DNA duplex at room temperature for 10 min, then adding $CdCl_2$, followed by additional 5 min incubation. All reaction mixtures (5 μl) were immediately loaded onto a 6% nondenaturing PAGE and electrophoresed for about 1 hr at 150 V using 1x TBE buffer.

**DNA Glycosylase Assay**. To test hAPNG-mediated cleavage of the same εA-containing oligomer as used in the binding assay, a DNA cleavage assay was carried out as described previously (*30, 32*). The reaction mixtures contained 2 nM $^{32}$P-end labeled oligomer duplex in 10 mM HEPES-KOH (pH 7.4), 100 mM KCl, 0.1 mM DTT, and varying amounts of purified hAPNG protein in a total volume of 10 μl. Metal ions were pre-incubated with hAPNG for 10 min on ice prior to the addition of the substrate DNA. Further incubations were carried out for 30 min at 37 °C. In reactions using cell-free extracts, 0.5 μg of poly(dI-dC)•poly(dI-dC) (Amersham Pharmacia Biotech, Piscataway,

NJ) was added to the reaction mixture as a nonspecific competitor. All the glycosylase reactions were stopped by adding 5 μl alkaline buffer (300 mM NaOH, 90% formamide, 0.05% bromophenol blue), followed by heating the samples at 95-100 °C for 3 min. Reaction products were resolved on a 7M urea 12% denaturing PAGE with a 5' $^{32}$P-labeled 5-mer marker. The gel was subsequently dried and scanned with the Bio-Rad FX Molecular PhosphorImager (Hercules, CA). For band quantitation, Quantity One software (version 4.0.1) was used according to the manufacturer's instructions. Data were plotted using CA-Cricket Graph III (Computer Associates, Islandia, NY) and Microsoft Excel 98.

**APE1 Nuclease Assay**. To test the metal inhibition of hAPE1 activity toward a THF-containing 25-mer oligonucleotide, a DNA cleavage assay as previously described (*33*) was used to detect the single strand breaks. Briefly, the standard reaction was performed in a mixture containing 2 nM $^{32}$P-end labeled oligomer duplex, 20 mM Tris-HCl (pH 7.4), 100 mM KCl, 1 mM $MgCl_2$ and varying concentrations of $ZnCl_2$ or $CdCl_2$ in a total volume of 10 μl. Initially, hAPE1 (0.38 nM) was pre-incubated with a metal ion for 10 min on ice. After the addition of the $^{32}$P-end labeled DNA substrate, the reaction was incubated at 37$^{o}$C for 10 min, stopped by addition of an equal volume of a gel loading buffer containing 50 mM EDTA, 90% formamide and 0.05% bromophenol blue. Gel electrophoresis, scanning and data analysis were performed as described above.

**Molecular Dynamics (MD) Simulations.** The starting coordinates for hAPNG were obtained from the hAPNG complexed to εA-containing DNA (PDB code id: 1f4r). All simulations were carried out using the SANDER module of Amber 8.0 (*34*) molecular modeling package with Cornell et al. force field (*35*). The force field parameters for the $Zn^{2+}$ atom were used from the Amber data set. Initially 4 $Cl^-$ ions were added to neutralize the system. Then, for the starting conformations, 10 $Zn^{2+}$ ions were randomly placed in the vicinity of the active site of the protein. Five sets of the initial models were prepared with different distribution of the metal ions around the active site. Figure 6 shows an example of one of the initial models. For each model the simulation consists of two steps, equilibration and production. During the equilibration the system was minimized for the 200 steps to remove any close contacts and relax atomic positions. The system was then gradually heated for 20 ps from 10 to 310 K using Langevin dynamics for temperature regulation while holding the solute fixed with harmonic restraints of 10 kcal $mol^{-1}Å^{-1}$. Unrestrained production MD runs were initiated after the equilibration steps and were carried out at 310 K for 1 ns. All calculations were performed with implicit solvent using generalized born simulations ($GB^{obc}$) using Bondi radii set (*36, 37*). The cutoff distance was set at 50 Å and a 1 fs time step was used for all simulations. The atomic coordinates were stored every 0.25 ps.

MD trajectories were processed using the CARNAL module of the Amber 8.0 package and visualized using VMD 1.8.3 software (*38*).

## Results and Discussion

Metals have long been known to be carcinogenic to humans and/or animals. Although many genotoxic and epigenetic effects have been identified for various metals, the precise mechanisms underlying such effects are still largely unknown. Recent data are emerging to suggest that metal-induced inhibition of DNA repair processes could play an important role, since impaired DNA repair capacity would directly lead to increased frequency of either spontaneous or environmentally induced mutagenesis, ultimately resulting in cancer. The reported weak mutagenic potential of metals *per se* and their comutagenicity with other genotoxic agents support such a notion.

As described in the Introduction, previous biochemical studies have identified several repair proteins that are targets for specific metal ions and their mechanisms of interactions proposed. In this study, we were interested in whether the activity of hAPNG, a BER enzyme that does not apparently require a metal for its function or structure, could be affected by the metal ions. *In vitro*, this enzyme is known to possess a broad substrate range which may have important biological implications (*25-27*). Given

that it is a major glycosylase activity excising alkylation damage, data obtained on metal inhibition of its activity may aid in understanding the molecular basis for the previously observed metal induced reduction in repair of DNA damage in cells exposed to alkylating agents (*20, 21*). In addition, available X-ray crystal structures of hAPNG complexed to DNA (*28, 29*) provided a structural framework for our modeling studies.

**Inhibition of hAPNG Activity by $Cd^{2+}$, $Zn^{2+}$ and $Ni^{2+}$.** Using an *in vitro* oligonucleotide-based cleavage assay, we have previously studied hAPNG activity towards the εA adduct and its analogues (*39-41*). In this work, to investigate possible inhibition of hAPNG by common metals, the same assay was utilized to test the activity of a recombinant hAPNG towards an oligonucleotide containing an εA, which is a product formed from the reaction of DNA with environmental carcinogens such as vinyl chloride or by internal metabolic processes such as lipid peroxidation (*25*). The glycosylase activity was tested at micromolar $Cd^{2+}$, $Ni^{2+}$, or $Zn^{2+}$ concentrations at 37°C for 30 min, followed by addition of an alkaline solution containing NaOH/formamide to cleave the resulting AP site. Separation of intact oligonucleotide (25-mer) and cleaved product (5-mer) was achieved with denaturing PAGE (details in the Experimental Procedures).

As shown in Figure 1, in the presence of $Cd^{2+}$ or $Zn^{2+}$, intensities of the expected 5-mer cleavage products (indicated by an arrow) decreased in a metal-dependent manner, and hAPNG lost more than 90% of activity when the concentration of both metal ions in the reaction mixture reaches 500 μM (Figure 2). When treated with $Ni^{2+}$, the cleavage activity of hAPNG also exhibited a concentration-dependent inhibition but to a lesser extent (Figures 1 and 2). For all three metals, partial reduction of hAPNG activity could be seen at their initial concentration, 50 μM, at which $Zn^{2+}$ is the most efficient inhibitor with an approximately 50% reduction of the hAPNG activity (Figure 2).

A key issue in these studies is to assess metal-induced effects at their environmentally and/or biologically relevant concentrations. For example, the concentrations of $Cd^{2+}$ in organs/tissues of healthy unexposed humans can be in the low to middle micromolar ranges. Studies showed that the levels of $Cd^{2+}$ reach 12-28 μM in the prostate, 0.9-6 μM in lungs, and significantly higher levels in kidneys and liver (*1, 42-44*). Under certain circumstances, levels of $Cd^{2+}$ could be significantly higher in cells. For instance, for cigarette smokers, the $Cd^{2+}$ concentrations can be 2-4 fold higher than in the non-smokers. Normally most of cellular $Cd^{2+}$ is bound to an intracellular protein called metallothionein (*45*). However, under oxidative stress, $Cd^{2+}$ may be released from this protein, leading to higher levels in the cell. Moreover, cadmium has a fairly long

biological half-life (10-30 years), thus resulting in age-dependent accumulation in organisms. In this work, the inhibition of APNG activity was observed at concentrations as low as 50 μM for all three metals tested. Based on the amounts of $Cd^{+2}$ in tissues described above, it is reasonable to speculate that such a level is biologically relevant.

A similar inhibition pattern was also observed when HeLa cell-free extracts were tested for activity against εA in the presence of $Cd^{2+}$, $Zn^{2+}$ or $Ni^{2+}$ (Figure 3). Since it was shown in our previous work the εA cleavage activity was virtually undetectable in tissues of APNG-knockout mice (*40*), the εA excision activity detected in Figure 3, using the same enzymatic assay, should reflect the activity of APNG in these extracts. Such experiments using cell-free extracts allow for assessment of any difference in inhibition between purified enzyme and cell-free extracts, as metal ions may interact with other protein component(s) in the extracts. In this study, the results obtained from using cell-free extracts are consistent with those from recombinant APNG with regard to metal specificity.

To investigate the effect of metal ions on hAPNG binding to the εA substrate, $Cd^{2+}$ at 125 to 2000 μM was added to binding reactions in two different ways. In Figure 4, Experiment 1, 140 nM hAPNG was pre-incubated with $Cd^{2+}$ for 10 min prior to the addition of εA-25-mer duplex. The result shows that hAPNG binding to this duplex was

not affected at concentrations ≤ 250 μM, slightly affected at 500 μM, suggesting that the greatly reduced catalytic activity of hAPNG observed in this range (Figure 2) is not due to altered APNG binding affinity for its substrate DNA. In Figure 4, Experiment 2, hAPNG and εA-25mer duplex were first incubated for 10 min at room temperature, followed by addition of $Cd^{2+}$ and further incubation for 5 min. Under this treatment, the extent of hAPNG binding to the DNA was not dramatically affected by the presence of $Cd^{2+}$ at concentrations ≤ 500 μM, indicating that $Cd^{2+}$ could not disrupt the already formed protein-DNA complex. In addition to proteins, $Cd^{2+}$ has the ability to bind to certain sites in DNA duplex, such as the N7 atoms of guanine residues, thus slightly destabilizing the DNA structure (*46*, *47*). In general, destabilization of the DNA helix could affect the initial formation of the hAPNG-DNA complex. However, our binding experiments showed that hAPNG binding to the DNA substrate is not affected significantly or proportionally at metal concentrations that exhibit catalytic inactivation. These results support the direct interaction between the metal and the protein catalytic element/function.

Similar to other repair proteins targeted by metals, the biological consequences of hAPNG inhibition identified from these biochemical experiments have yet to be determined. APNG is the major DNA glycosylase that removes cytotoxic and mutagenic

alkylated bases (*26, 27*). Previous studies using mammalian cells have shown that metals such as $Cd^{2+}$ inhibit repair of DNA damage formed by alkylating agents such as methyl methanesulfonate (MMS) and *N*-methyl-*N*-nitrosourea (MNU) (*20, 21*). These chemicals are potent human carcinogens and capable of forming a variety of alkylated bases, many of which are recognized and excised by the APNG protein. Therefore, it is reasonable to propose that the inhibition of APNG activity by metals contributes to such metal induced decrease in the cellular repair of alkylation DNA damage.

It was recently reported by McNeill *et al.* (*17*) that $Pb^{2+}$, $Fe^{2+}$ and $Cd^{2+}$ inhibit the nuclease activity of hAPE1, a pivotal enzyme in BER that processes the AP sites generated by DNA glycosylases or formed spontaneously (*10, 48*). Therefore, both hAPNG glycosylase activity and hAPE1 nuclease activity can be inhibited *in vitro* by the same metal ion, $Cd^{2+}$. Since APE1 is responsible for >95% of the total AP endonuclease activity in human cell extracts (*49*), it could be argued that the inhibition of APE1 by $Cd^{+2}$ *in vivo* would block the majority of BER capacity regardless of whether APNG is inhibited or not. However, the inactivation of APE1 yields accumulation of AP sites, whereas inhibition of the APNG activity would result in accumulation of a variety of modified base lesions, which may cause differential effects on DNA structure and function than an AP site. In the case of $Ni^{2+}$, it inhibits the activity of hAPNG (this work) but not that of hAPE1 (*17*), showing a different inhibition specificity than $Cd^{+2}$. In this

study, we were also curious about whether the $Zn^{2+}$ ion inhibits the AP endonuclease activity of hAPE1. As shown in Figure 5, at the concentrations tested, $Zn^{+2}$ showed a metal-dependent inhibition of the activity of hAPE1 towards DNA containing a synthetic AP site THF, indicating that $Zn^{2+}$, similar to $Cd^{+2}$, can also suppress the activity of both proteins. It should be noted that, in the case of APE1 inhibition, BER may be able to bypass it through another enzyme, the polynucleotide kinase (PNK), as shown for the human endonuclease VIII-like glycosylase 1 (NEIL1) (*50*). However, caution should be exercised in extrapolating data from *in vitro* to *in vivo*, as many factors could affect the reaction conditions and pathway regulations when metal inhibition takes place in cells.

**Molecular Dynamics Simulations of Interaction of hAPNG with $Zn^{2+}$**. Previous studies suggested that inhibition of repair proteins is mainly associated with displacement by environmental metals of the original metal ions utilized by proteins for their function or structure. In interactions with zinc finger proteins such as XPA (*19, 51, 52*), metal ions like $Cd^{2+}$ and $Ni^{2+}$ have a high affinity for the –SH groups and can replace or compete with $Zn^{2+}$ at the Cys-His motifs. Simultaneous treatment with $Zn^{2+}$ can partially prevent inhibition by $Cd^{2+}$ or $Ni^{2+}$. For hAPE1, which requires $Mg^{2+}$ in its catalytic mechanisms proposed from structural studies (*53-55*), the inhibitory metals may occupy the $Mg^{2+}$ binding sites but with different coordination chemistry or ligand preferences, thus disrupting the $Mg^{2+}$-dependent catalysis (*17*). The mechanism of inhibition of the ATPase

activity of MSH2-MSH6 by $Cd^{2+}$ is not clear, even though $Mg^{2+}$ is an element at the ATPase active site. It was proposed that $Cd^{2+}$ could bind to other site(s) in these proteins through coordination with specific residues in tetrahedral geometries (*14*, *15*).

To gain insight into the mechanism of hAPNG-metal interaction, we performed MD simulations using $Zn^{2+}$ as a representative cation. The 3D protein structure was based on the coordinates from the previously reported crystal structure of hAPNG (*29*). As shown in Figure 6, the $Zn^{2+}$ ions, when located in a close proximity to the enzyme active site, have the ability to protrude into the active site, showing higher affinity for the negatively charged groups of the residues lining the cavity walls. In 3 out of 5 starting conformations, one of the $Zn^{2+}$ ions initially interacted with the negatively charged main chain carbonyl groups of Gly 249 and Val 248. This interaction took place after first 20 ps of MD simulation. However, the position of the metal was rather unstable at this site and it further moved toward the anionic patch formed by the side chain of Glu 125 and O from the hydroxyl group of Tyr 127. The position of the metal ion was stabilized at this site for the rest of the simulation. In the final conformation, the $Zn^{2+}$ ion is coordinated with the side chains of Glu 125 and Tyr 127, the main chain carbonyl group of Val 248 and the O of the active site water molecule, thus providing a template for the tetrahedral coordination of the metal ion (Figure 7). Such a tetrahedral coordination is a preferred

coordination for $Zn^{2+}$ among 309 structures analyzed from the Metalloprotein Database and Browser (MBD) (*56*).

Based on the above data, we propose that the hAPNG active site pocket could have a binding site for the positively charged metal ions such as $Zn^{2+}$ or $Cd^{2+}$. However, in order for metal ions to bind to this site they have to be close to the active site, which can be achieved at elevated concentrations of the metal. For example, in our biochemical experiments shown in Figure 1, at 50 μM $Zn^{2+}$ and 350 nM hAPNG, the ratio of the metal to protein is 142:1, which is a substantial excess of the metal ions over the APNG molecules in solution. The binding of the metal to the conserved active site residues such as Glu 125 and Tyr 127 is expected to interfere with the catalytic mechanism of hAPNG. It has previously been proposed that the Glu 125 abstracts a proton from a water molecule, thus generating nucleophile ($OH^-$) which attacks the glycosylic bond (*28, 29*). Displacement of water at the active site by a positively charged metal or precluding the water interaction with Glu 125 could result in the loss of the essential nucleophile for the catalytic reaction.

In our simulation studies $Zn^{2+}$ was used as a model ion, since it showed an efficient inactivation of the hAPNG activity (Figures 1 and 2) and its parameters are available in Amber force field. As far as $Cd^{2+}$ is concerned, it is known that $Cd^{2+}$ has a high affinity

toward $Zn^{2+}$ binding sites in metalloproteins motifs (*57-59*). Analysis of the $Cd^{2+}$ binding sites in metalloproteins suggested that this metal has a preference for the Cys, Glu, Asp and His residues in tetrahedral geometries (*8, 56*), thus suggesting that the $Zn^{2+}$ binding site identified in our modeling could also be bound by $Cd^{2+}$. The lower inhibition of the hAPNG activity by $Ni^{2+}$ relative to $Cd^{2+}$ and $Zn^{2+}$ (Figure 2) may be correlated with the data showing that $Ni^{2+}$ prefers coordination through 5 to 6 ligands, based on the analysis of available structures in MDB (*56*), while the hAPNG metal binding site proposed from our modeling favors tetrahedral coordination.

## Conclusion

Inhibition of DNA repair has recently been considered as a contender for the mechanism underlying the metal-induced mutagenesis and carcinogenesis. Consistent with this, the work reported here indicates that $Cd^{2+}$, $Ni^{2+}$ and $Zn^{2+}$ can inhibit the catalytic activity of hAPNG at submillimolar concentrations, which could enhance gentotoxic potential of a variety of compounds such as alkylating agents. Although *in vitro* work on metal inhibition allows mechanistic insight into operation of this enzyme in cellular repair processes, further *in vivo* studies are needed to assess the biological implications of these biochemical inhibitory effects, such as the role of APNG in metal induced suppression of repair of DNA damage caused by alkylating agents in cells.

Mechanistically, the finding that a non-metal requiring repair enzyme like hAPNG can be inhibited by metal ions is worth to be explored with other enzymes that have a similar nature. Molecular dynamics simulations provide a first insight into potential interactions between metal ion and the active site of hAPNG. Future work towards understanding the chemical details of such interactions would be essential for elucidating the precise mechanism of metal inhibition.

**Acknowledgements.** This work was supported by NIH grant CA72079 (to B.H.) and was administrated by the Lawrence Berkeley National Laboratory under Department of Energy contract DE-AC03-76SF00098.

**References**


(1) U.S. Department of Health and Human Services. (2005) National Toxicology Program.

(2) IARC. (1993) Beryllium, cadmium, mercury and exposures in the glass manufacturing industry., in *International Agency for Research on Cancer Monographs on the Evaluation of Carcinogenic Risks of Chemicals to Humans*, IARC Scientific Publications, Lyon.

(3) IARC. (1990) Chromium, Nickel and Welding, in *International Agency for Research on Cancer Monographs on the Evaluation of Carcinogenic Risks of Chemical to Humans*, IARC Scientific Publications, Lyon.

(4) Vallee, B. L., and Falchuk, K. H. (1993) The biochemical basis of zinc physiology. *Physiol Rev 73*, 79-118.

(5) Agency for Toxic Substances and Disease Registry (ATSDR), U.S. Department of Health and Human Services. (2005) Public Health Service., Atlanta.

(6) Durham, T. R., and Snow, E. T. (2006) Metal ions and carcinogenesis. *Exs 96*, 97-130.

(7) Waisberg, M., Joseph, P., Hale, B., and Beyersmann, D. (2003) Molecular and cellular mechanisms of cadmium carcinogenesis. *Toxicology 192*, 95-117.

(8) McMurray, C. T., and Tainer, J. A. (2003) Cancer, cadmium and genome integrity. *Nat Genet 34*, 239-41.

(9) Hartwig, A., and Schwerdtle, T. (2002) Interactions by carcinogenic metal compounds with DNA repair processes: toxicological implications. *Toxicol Lett 127*, 47-54.

(10) Friedberg, E. C., Walker, G. C., Siede, W., Wood, R. D., Schultz, R. A., and Ellenberger, T. (2005) *DNA Repair and Mutagenesis*, 2nd ed., ASM Press.

(11) Wood, R. D., Mitchell, M., and Lindahl, T. (2005) Human DNA repair genes, 2005. *Mutat Res 577*, 275-83.

(12) Asmuss, M., Mullenders, L. H., Eker, A., and Hartwig, A. (2000) Differential effects of toxic metal compounds on the activities of Fpg and XPA, two zinc finger proteins involved in DNA repair. *Carcinogenesis 21*, 2097-104.

(13) Kopera, E., Schwerdtle, T., Hartwig, A., and Bal, W. (2004) Co(II) and Cd(II) substitute for Zn(II) in the zinc finger derived from the DNA repair protein XPA, demonstrating a variety of potential mechanisms of toxicity. *Chem Res Toxicol 17*, 1452-8.

(14) Clark, A. B., and Kunkel, T. A. (2004) Cadmium inhibits the functions of eukaryotic MutS complexes. *J Biol Chem 279*, 53903-6.

(15) Banerjee, S., and Flores-Rozas, H. (2005) Cadmium inhibits mismatch repair by blocking the ATPase activity of the MSH2-MSH6 complex. *Nucleic Acids Res 33*, 1410-9.

(16) Zharkov, D. O., and Rosenquist, T. A. (2002) Inactivation of mammalian 8-oxoguanine-DNA glycosylase by cadmium(II): implications for cadmium genotoxicity. *DNA Repair (Amst) 1*, 661-70.

(17) McNeill, D., Narayana, A., Wong, H., and Wilson, D. M., 3rd. (2004) Inhibition of Ape1 Nuclease Activity by Lead, Iron and Cadmium. *Toxigenomics 112*, 799-804.

(18) Popenoe, E. A., and Schmaeler, M. A. (1979) Interaction of human DNA polymerase beta with ions of copper, lead, and cadmium. *Arch Biochem Biophys. 196*, 109-20.

(19) Hartwig, A., Asmuss, M., Blessing, H., Hoffmann, S., Jahnke, G., Khandelwal, S., Pelzer, A., and Burkle, A. (2002) Interference by toxic metal ions with zinc-dependent proteins involved in maintaining genomic stability. *Food Chem Toxicol 40*, 1179-84.

(20) Fatur, T., Lah, T. T., and Filipic, M. (2003) Cadmium inhibits repair of UV-, methyl methanesulfonate- and N-methyl-N-nitrosourea-induced DNA damage in Chinese hamster ovary cells. *Mutat Res 529*, 109-16.

(21) Hartmann, A., and Speit, G. (1994) Comparative investigations of the genotoxic effects of metals in the single cells gel (SCG) assay and the sister chromatid exchange (SCE) test. *Environ Mol Mutagen 23*, 299-305.

(22) Potts, R. J., Bespalov, I. A., Wallace, S. S., Melamede, R. J., and Hart, B. A. (2001) Inhibition of oxidative DNA repair in cadmium-adapted alveolar epithelial cells and the potential involvement of metallothionein. *Toxicology 161*, 25-38.

(23) Dally, H., and Hartwig, A. (1997) Induction and repair inhibition of oxidative DNA damage by nickel(II) and cadmium(II) in mammalian cells. *Carcinogenesis 18*, 1021-6.

(24) Hartwig, A., Pelzer, A., Asmuss, M., and Burkle, A. (2003) Very low concentrations of arsenite suppress poly(ADP-ribosyl)ation in mammalian cells. *Int J Cancer 104*, 1-6.

(25) Hang, B. (2004) Repair of exocyclic DNA adducts: rings of complexity. *Bioessays 26*, 1195-208.

(26) Wyatt, M. D., Allan, J. M., Lau, A. Y., Ellenberger, T. E., and Samson, L. (1999) 3-methyladenine DNA glycosylases: structure, function, and biological importance. *Bioessays 2*, 668-76.

(27) Memisoglu, A., and Samson, L. (2000) Base excision repair in yeast and mammals. *Mutat Res 451*, 39-51.

(28) Lau, A. Y., Scharer, O. D., Samson, L., Verdine, G. L., and Ellenberger, T. (1998) Crystal structure of a human alkylbase-DNA repair enzyme complexed to DNA: mechanisms for nucleotide flipping and base excision. *Cell 95*, 249-58.

(29) Lau, A. Y., Wyatt, M. D., Glassner, B. J., Samson, L. D., and Ellenberger, T. (2000) Molecular basis for discriminating between normal and damaged bases by the human alkyladenine glycosylase, AAG. *Proc Natl Acad Sci U S A 97*, 13573-8.

(30) Hang, B., Medina, M., Fraenkel-Conrat, H., and Singer, B. (1998) A 55-kDa protein isolated from human cells shows DNA glycosylase activity toward 3,$N^4$-ethenocytosine and the G/T mismatch. *Proc Natl Acad Sci U S A 95*, 13561-6.

(31) Dosanjh, M. K., Chenna, A., Kim, E., Fraenkel-Conrat, H., Samson, L., and Singer, B. (1994) All four known cyclic adducts formed in DNA by the vinyl chloride metabolite chloroacetaldehyde are released by a human DNA glycosylase. *Proc Natl Acad Sci U S A 91*, 1024-8.

(32) Hang, B., Downing, G., Guliaev, A. B., and Singer, B. (2002) Novel activity of Escherichia coli mismatch uracil-DNA glycosylase (Mug) excising 8-

(hydroxymethyl)-3,$N^4$-ethenocytosine, a potential product resulting from glycidaldehyde reaction. *Biochemistry 41*, 2158-65.

(33) Sagi, J., Hang, B., and Singer, B. (1999) Sequence-dependent repair of synthetic AP sites in 15-mer and 35-mer oligonucleotides: role of thermodynamic stability imposed by neighbor bases. *Chem Res Toxicol 12*, 917-23.

(34) Case, D. A., Pearlman, D. A., Caldwell, J. W., Cheatham, T. E., Wang, J., Ross, W. S., Simmerling, C. L., Darden, T. A., Merz, K. M., Stanton, R. V., Cheng, A. L., Vincent, J. J., Crowley, M., Tsui, V., Radmer, R. J., Gohlke, H., Duan, Y., Pitera, J., Massova, I., Seibel, G. L., Singh, U. C., Weiner, P. K., and Kolman, P. A. (2004) AMBER 8. *University of California, San Francisco*.

(35) Cornell, W. D., Cieplak, P., Bayly, C. I., Gould, I. R., Merz, K., Ferguson, D., Spellmeyer, D., Fox, T., Caldwell, J. W., and Kolman, P. A. (1995) A second generation force field for the simultaion of proteins, nucleic acids, and organic molecules. *J. Am. Chem. Soc. 117*, 5179-5197.

(36) Onufriev, A., Bashford, D., and Case, D. A. (2000) Modification of the Generalized Born Model Suitable for the Macromolecules. *J. Phys. Chem. B 104*, 3712-3720.

(37) Feig, M., Onufriev, A., Lee, M. S., Im, W., Case, D. A., and Brooks, C. L., 3rd. (2004) Performance comparison of generalized born and Poisson methods in the calculation of electrostatic solvation energies for protein structures. *J Comput Chem 25*, 265-84.

(38) Humphrey, W., Dalke, A., and Schulten, K. (1996) VMD - Visual Molecular Dynamics. *J. Molec. Graphics 14*, 33-38.

(39) Wang, P., Guliaev, A. B., Elder, R. H., and Hang, B. (2006) Alkylpurine-DNA-N-glycosylase excision of 7-(hydroxymethyl)-1,$N^6$-ethenoadenine, a glycidaldehyde-derived DNA adduct. *DNA Repair (Amst) 5*, 23-31.

(40) Hang, B., Singer, B., Margison, G. P., and Elder, R. H. (1997) Targeted deletion of alkylpurine-DNA-N-glycosylase in mice eliminates repair of 1,$N^6$-ethenoadenine and hypoxanthine but not of 3,$N^4$-ethenocytosine or 8-oxoguanine. *Proc Natl Acad Sci U S A 94*, 12869-74.

(41) Guliaev, A. B., Hang, B., and Singer, B. (2002) Structural insights by molecular dynamics simulations into differential repair efficiency for ethano-A versus etheno-A adducts by the human alkylpurine-DNA N-glycosylase. *Nucleic Acids Res 30*, 3778-87.

(42) Barregard, L., Svalander, C., Schutz, A., Westberg, G., Sallsten, G., Blohme, I., Molne, J., Attman, P. O., and Haglind, P. (1999) Cadmium, mercury, and lead in kidney cortex of the general Swedish population: a study of biopsies from living kidney donors. *Environ Health Perspect 107*, 867-71.

(43) Jin, Y. H., Clark, A. B., Slebos, R. J., Al-Refai, H., Taylor, J. A., Kunkel, T. A., Resnick, M. A., and Gordenin, D. A. (2003) Cadmium is a mutagen that acts by inhibiting mismatch repair. *Nat Genet 34*, 326-9.

(44) Fribergh, L., Elinder, C. G., Kjellstrom, T., Nordbergh, G. F. (1985) *Cadmium and Health: A Toxicological and Epidemiologcal Apprasial*, Vol. 1, CRC Press, Inc., Boca Raton, Florida.

(45) Klaassen, C. D., Liu, J., and Choudhuri, S. (1999) Metallothionein: an intracellular protein to protect against cadmium toxicity. *Annu Rev Pharmacol Toxicol 39*, 267-94.

(46) Duguid, J. G., Bloomfield, V. A., Benevides, J. M., and Thomas, G. J., Jr. (1995) Raman spectroscopy of DNA-metal complexes. II. The thermal denaturation of DNA in the presence of $Sr^{2+}$, $Ba^{2+}$, $Mg^{2+}$, $Ca^{2+}$, $Mn^{2+}$, $Co^{2+}$, $Ni^{2+}$, and $Cd^{2+}$. *Biophys J 69*, 2623-41.

(47) Duguid, J., Bloomfield, V. A., Benevides, J., and Thomas, G. J., Jr. (1993) Raman spectroscopy of DNA-metal complexes. I. Interactions and conformational effects of the divalent cations: Mg, Ca, Sr, Ba, Mn, Co, Ni, Cu, Pd, and Cd. *Biophys J 65*, 1916-28.

(48) Wilson, D. M., 3rd, and Barsky, D. (2001) The major human abasic endonuclease: formation, consequences and repair of abasic lesions in DNA. *Mutat Res 485*, 283-307.

(49) Demple, B., Herman, T., and Chen, D. S. (1991) Cloning and expression of APE, the cDNA encoding the major human apurinic endonuclease: definition of a family of DNA repair enzymes. *Proc Natl Acad Sci U S A 88*, 11450-4.

(50) Wiederhold, L., Leppard, J. B., Kedar, P., Karimi-Busheri, F., Rasouli-Nia, A., Weinfeld, M., Tomkinson, A. E., Izumi, T., Prasad, R., Wilson, S. H., Mitra, S., and Hazra, T. K. (2004) AP endonuclease-independent DNA base excision repair in human cells. *Mol Cell 15*, 209-20.

(51) Witkiewicz-Kucharczyk, A., and Bal, W. (2005) Damage of zinc fingers in DNA repair proteins, a novel molecular mechanism in carcinogenesis. *Toxicol Lett*.

(52) Buchko, G. W., Hess, N. J., and Kennedy, M. A. (2000) Cadmium mutagenicity and human nucleotide excision repair protein XPA: CD, EXAFS and (1)H/(15)N-NMR spectroscopic studies on the zinc(II)- and cadmium(II)-associated minimal DNA-binding domain (M98-F219). *Carcinogenesis 21*, 1051-7.

(53) Beernink, P. T., Segelke, B. W., Hadi, M. Z., Erzberger, J. P., Wilson, D. M., 3rd, and Rupp, B. (2001) Two divalent metal ions in the active site of a new crystal form of human apurinic/apyrimidinic endonuclease, Ape1: implications for the catalytic mechanism. *J Mol Biol 307*, 1023-34.

(54) Lowry, D. F., Hoyt, D. W., Khazi, F. A., Bagu, J., Lindsey, A. G., and Wilson, D. M., 3rd. (2003) Investigation of the role of the histidine-aspartate pair in the human exonuclease III-like abasic endonuclease, Ape1. *J Mol Biol 329*, 311-22.

(55) Mol, C. D., Izumi, T., Mitra, S., and Tainer, J. A. (2000) DNA-bound structures and mutants reveal abasic DNA binding by APE1 and DNA repair coordination [corrected]. *Nature 403*, 451-6.

(56) Castagnetto, J. M., Hennessy, S. W., Roberts, V. A., Getzoff, E. D., Tainer, J. A., and Pique, M. E. (2002) MDB: the Metalloprotein Database and Browser at The Scripps Research Institute. *Nucleic Acids Res 30*, 379-82.

(57) Laity, J. H., Lee, B. M., and Wright, P. E. (2001) Zinc finger proteins: new insights into structural and functional diversity. *Curr Opin Struct Biol 11*, 39-46.

(58) Hopfner, K. P., Craig, L., Moncalian, G., Zinkel, R. A., Usui, T., Owen, B. A., Karcher, A., Henderson, B., Bodmer, J. L., McMurray, C. T., Carney, J. P., Petrini, J. H., and Tainer, J. A. (2002) The Rad50 zinc-hook is a structure joining Mre11 complexes in DNA recombination and repair. *Nature 418*, 562-6.

(59) Hartwig, A. (2001) Zinc finger proteins as potential targets for toxic metal ions: differential effects on structure and function. *Antioxid Redox Signal 3*, 625-34.

**Figure legends**

Figure 1. Cleavage assay of recombinant hAPNG against a 25-mer oligonucleotide containing an εA adduct under various concentrations of metal ions. Standard enzymatic reactions were carried out at 37°C for 30 min under conditions described in Experimental Procedures. The reactions were terminated by addition 5 μl of an alkaline solution (NaOH/formamide) to 10 μl of the reaction mixture, followed by heating samples at100°C for 3 min to cleave the AP sites generated by hAPNG. The arrow indicates the migration position of the 5-mer marker which is the expected position of a cleavage product. Lane 1 contained buffer only. Lane 2 contained purified hAPNG without a metal ion.

Figure 2. Relative cleavage activity of hAPNG towards εA under various concentrations of metal ions. For quantitation of the bands corresponding to the cleaved product and the remaining uncut substrate, band areas on the phosphorimage were measured by Quantity One software (version 4.0.1). The activity of hAPNG for εA without the presence of metal ions was treated as 100%. Experimental conditions were as described in Figure 1. The data were an average value of three parallel experiments.

Figure 3. Cleavage assay of HeLa cell-free extracts toward the εA-containing oligonucleotide under various concentrations of metal ions. The reactions were carried out at 37°C for 1 hr under conditions described in Experimental Procedures and stopped by addition of 5 μl NaOH/formamide and heating at 95°C for 3 min to cleave the AP sites. The latter procedure is normally not required for assaying glycosylase-mediated cleavage since HeLa cell-free extracts contain sufficient AP endonuclease activity to hydrolyze the AP sites. However, in this study, the original APE activity in extracts could be inhibited by metal ions.

Figure 4. Gel mobility shift assay of hAPNG binding to the 25-mer oligonucleotide containing an εA adduct. Top gel image: DNA bound to hAPNG and unbound DNA were labeled as "Bound" and "Free DNA", respectively. Experiment 1: Pre-incubation of 140 nM hAPNG with varying concentrations of $Cd^{2+}$ on ice for 10 min, followed by addition of 2 nM $^{32}$P-labelled DNA and incubation at room temperature (~20°C) for 15 min. Experiment 2: Incubation of 140 nM hAPNG with 2 nM DNA at room temperature for 10 min followed by addition of $Cd^{2+}$ and further incubation for 5 min. All reactions were immediately loaded onto a 6% non-denaturing PAGE. Bottom bar graphs: The bands labeled “Bound” and “Free DNA” in both Experiments 1 and 2 were scanned and

plotted as % hAPNG binding to the DNA substrate. The left graph is corresponding to Experiment 1 in top gel image and the right graph is corresponding to Experiment 2.

Figure 5. Effect of $Zn^{2+}$ and $Cd^{2+}$ on the AP activity of hAPE1 using the 25-mer oligonucleotide containing a THF. Pre-incubation of hAPE1 with a metal ion and standard enzymatic reactions were described in Experimental Procedures. The arrow on the right side of the top gel image indicates the 7-mer cleavage product from hAPE1. The bottom bar graph shows the relative cleavage activity of hAPE1 under various $Zn^{2+}$ concentrations. For comparison, $Cd^{2+}$, which is known to inhibit hAPE1 (*17*), was tested in parallel with $Zn^{2+}$ under the same conditions. The activity of APE1 without the presence of a metal ion is designated as 100%.

Figure 6. Representative starting conformation used for the MD simulation of hAPNG with 10 $Zn^{2+}$ cations distributed around the active site. The catalytically important active site residues are colored by atom. $Zn^{2+}$ cations are shown as light blue spheres. $Cl^-$ counterions are shown as green spheres.

Figure 7. The position of the $Zn^{2+}$ ion at the hAPNG active site as determined by 1ns MD simulations. The $Zn^{2+}$ ion (shown in light blue sphere) is coordinated by the side chains

of Glu 125 and Tyr 127, and the main chain carbonyl of Val 248. In addition, the metal ion is coordinated by the O of the active site water molecule.

Figure 1

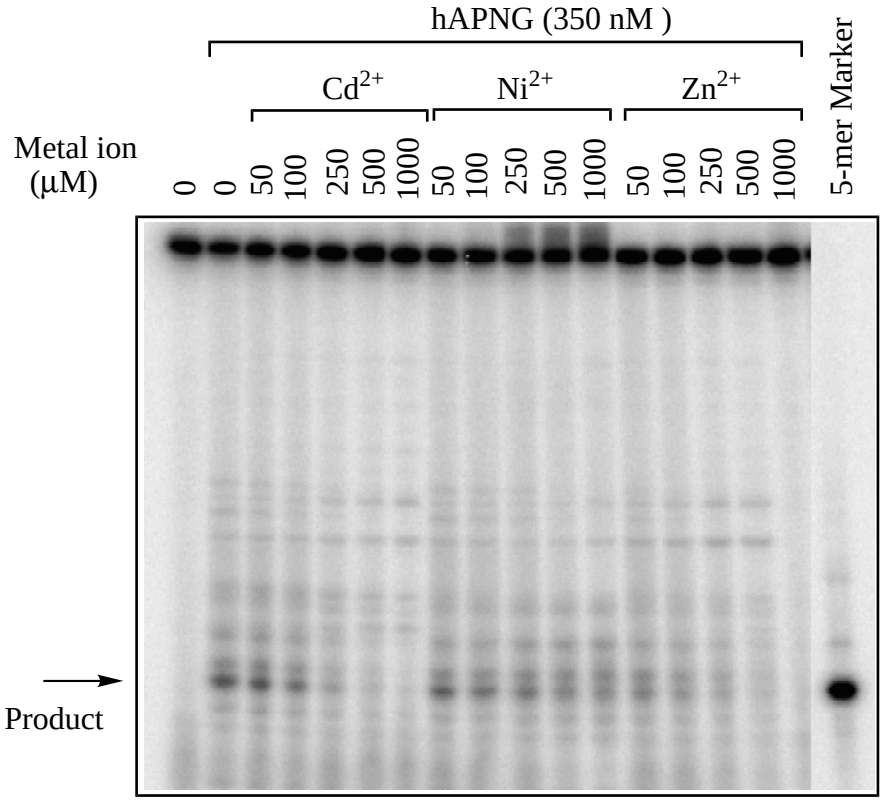
hAPNG (350 nM )
Cd2+
Ni2+
Zn2+
Metal ion (μM)
0
0
50
100
250
500
1000
50
100
250
500
1000
50
100
250
500
1000
5-mer Marker
Product

Figure 2

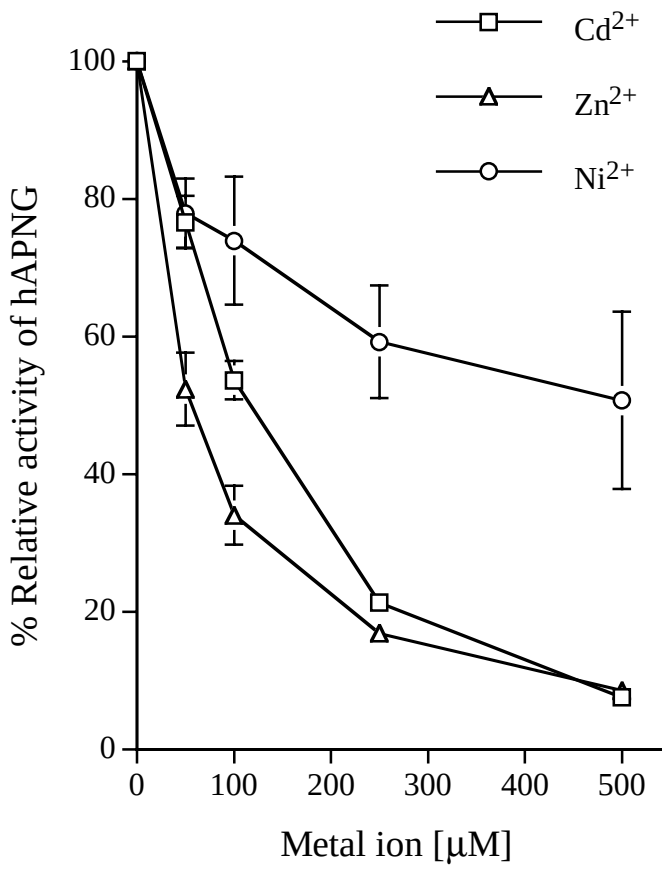
Cd2+
Zn2+
Ni2+
100
80
60
40
20
0
% Relative activity of hAPNG
0
100
200
300
400
500
Metal ion [μM]

Figure 3

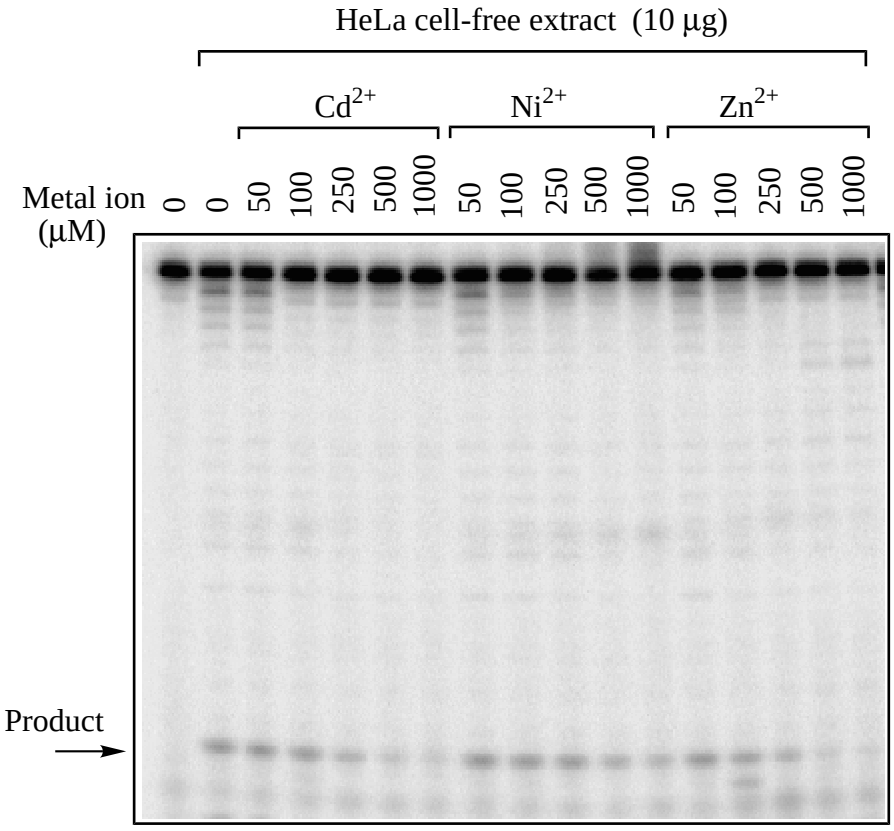
HeLa cell-free extract (10 μg)
Cd2+
Ni2+
Zn2+
Metal ion (μM)
0
0
50
100
250
500
1000
50
100
250
500
1000
50
100
250
500
1000
Product

Figure 4

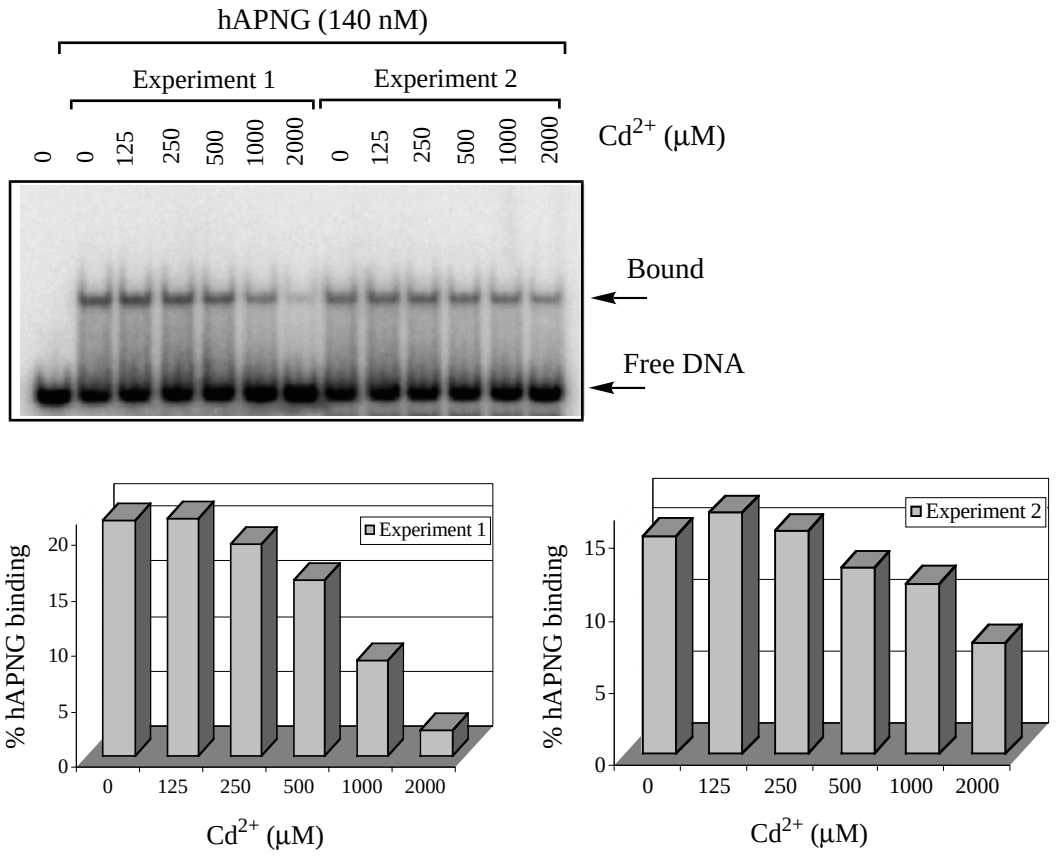
hAPNG (140 nM)
Experiment 1
Experiment 2
0
0
125
250
500
1000
2000
0
125
250
500
1000
2000
Cd2+ (μM)
Bound
Free DNA
% hAPNG binding
Experiment 1
0
5
10
15
20
0
125
250
500
1000
2000
Cd2+ (μM)
% hAPNG binding
Experiment 2
0
5
10
15
0
125
250
500
1000
2000
Cd2+ (μM)

Figure 5

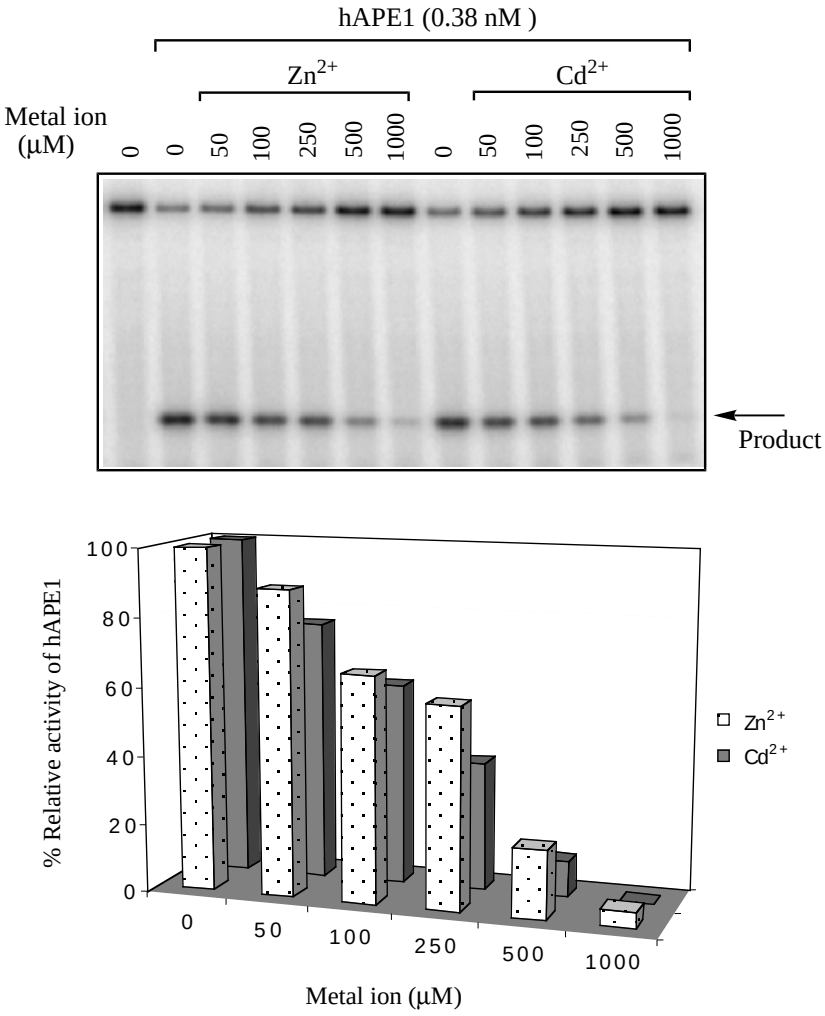
hAPE1 (0.38 nM )
Zn2+
Cd2+
Metal ion (μM)
0
0
50
100
250
500
1000
0
50
100
250
500
1000
Product
% Relative activity of hAPE1
100
80
60
40
20
0
0
50
100
250
500
1000
Metal ion (μM)
Zn2+
Cd2+

Figure 6

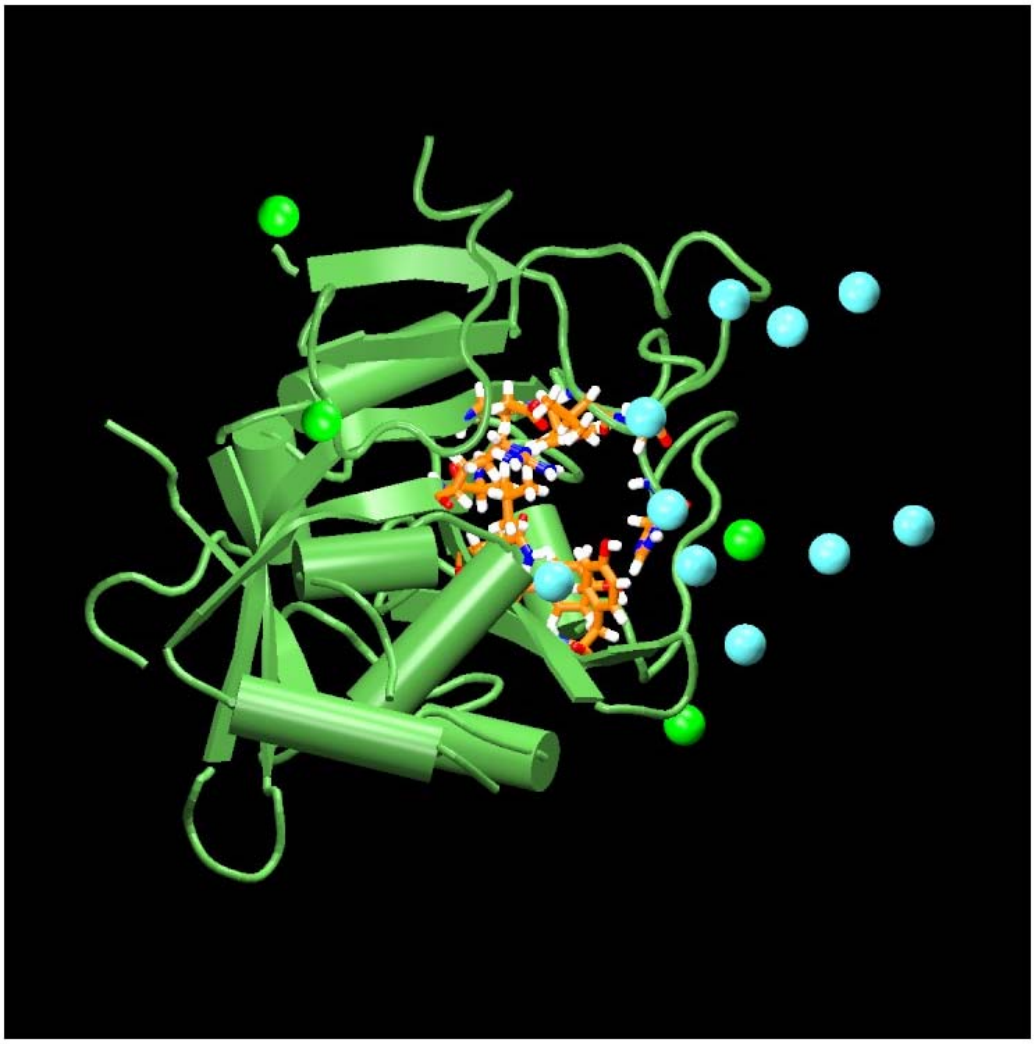

Figure 7